




An alternatively transcribed TAZ variant negatively regulates JAK-STAT signaling

Chuantao Fang¹, Jian Li¹, Sixian Qi¹, Yubin Lei¹, Yan Zeng¹, Pengcheng Yu^{2,3}, Zhaolan Hu⁴, Yufeng Zhou¹, Yulong Wang^{2,3}, Ruping Dai⁴, Jin Li¹, Shenglin Huang⁵, Pinglong Xu⁶ , Kang Chen^{7,8,9}, Chen Ding¹⁰ & Fa-Xing Yu^{1,*}

Abstract

Type I interferon (IFN)-induced Janus kinase (JAK)–signal transducer and activator of transcription (STAT) signaling drives the expression of IFN-stimulated genes (ISGs) to mediate antiviral response. The strength and duration of JAK-STAT signaling are tightly regulated to ensure effective antiviral defense while avoiding pathological inflammation and autoimmunity. Here, we report that cTAZ, an isoform of the Hippo pathway effector TAZ, is transcribed by an alternative promoter. Although majority of C-terminal sequences of TAZ is retained, cTAZ is not regulated by the Hippo signaling and does not mediate its growth-inhibitory functions. Instead, cTAZ negatively regulates JAK-STAT signaling by inhibiting STAT1/2 nuclear localization and ISG expression, and its expression is induced by type I IFN. Thus, cTAZ functions as a modulator of JAK-STAT signaling and may play a role in fine-tuning cellular antiviral response.

Keywords alternative transcript; Hippo pathway; JAK-STAT pathway; viral infection

Subject Categories Immunology; Microbiology, Virology & Host Pathogen Interaction; Signal Transduction

DOI 10.15252/embr.201847227 | Received 12 October 2018 | Revised 25 March 2019 | Accepted 25 March 2019 | Published online 11 April 2019

EMBO Reports (2019) 20: e47227

See also: **S Strano & G Blandino** (June 2019)

Introduction

Type I interferons (IFNs), consisting mainly of IFN- α and IFN- β , are cytokines produced upon microbial infections to activate both innate

immunity and adaptive immunity [1]. Mutations in components of the type I IFN signaling pathway frequently lead to immunodeficiency and susceptibility to infection [2]. Type I IFNs have been developed as therapeutic agents to treat viral infections and various cancers [3,4]. However, prolonged type I IFNs' exposure can lead to autoimmune diseases, such as systemic lupus erythematosus [5]. Thus, the activity of type I IFN signaling should be tightly controlled.

Type I IFNs exert their biological functions through the Janus kinase (JAK)–signal transducer and activator of transcription (STAT) signaling pathway. Briefly, upon type I IFNs binding to their transmembrane receptors, type I IFNs trigger the activation of receptor-associated JAKs, which in turn phosphorylate STAT1 and STAT2. Phosphorylated STAT1 and STAT2 dimerize and translocate into nucleus and form a trimeric complex with IFN-regulatory factor 9 (IRF9). This complex specifically binds to the promoters containing IFN-sensitive response elements (ISREs) to drive the transcription of IFN-stimulated genes (ISGs) [6–8]. The strength of type I IFN response is modulated at multiple levels. The expression of type I IFNs is mainly regulated by IRFs, such as IRF3 and IRF7 [9–11]. IRF3/7 integrates upstream signaling from membrane-associated Toll-like receptors and cytosolic nucleic acid sensors, such as AIM2-like receptors and RIG-I-like receptors, to induce transcription of type I IFNs [10,12,13]. Meanwhile, *IRF7* is a direct target gene of STAT proteins, which constitutes a positive feedback mechanism of JAK-STAT signaling by enhancing type I IFN production [9,14]. Moreover, JAK-STAT signaling can be modulated by ISGs directly. For instance, ISGs such as *STAT1*, *STAT2*, and *IRF9*, positively regulate JAK-STAT signaling. On the other hand, ISGs, including suppressor of cytokine signaling 1/3 (*SOCS1/3*) and ubiquitin-specific peptidase 18 (*USP18*), negatively regulate JAK-STAT signaling [13,15]. Hence, JAK-STAT signaling is regulated by both positive and negative feedback mechanisms to meet the requirement of host tissues.

¹ Children's Hospital and Institutes of Biomedical Sciences, Key Laboratory of Medical Epigenetics and Metabolism, Fudan University, Shanghai, China

² Department of Head and Neck Surgery, Fudan University Shanghai Cancer Center, Shanghai, China

³ Department of Oncology, Shanghai Medical College, Fudan University, Shanghai, China

⁴ Department of Anesthesiology, The Second Xiangya Hospital, Central South University, Changsha, China

⁵ Fudan University Shanghai Cancer Center, Institutes of Biomedical Sciences, Shanghai Medical College, Fudan University, Shanghai, China

⁶ Life Sciences Institute and Innovation Center for Cell Signaling Network, Zhejiang University, Hangzhou, China

⁷ Perinatology Research Branch, Eunice Kennedy Shriver NICHD, National Institutes of Health, Detroit, MI, USA

⁸ Department of Obstetrics and Gynecology, Wayne State University, Detroit, MI, USA

⁹ Jiangsu Province Hospital of TCM, The Affiliated Hospital of Nanjing University of TCM, Nanjing, China

¹⁰ State Key Laboratory of Genetic Engineering, Human Phenome Institute, Institutes of Biomedical Sciences, School of Life Sciences, Zhongshan Hospital, Fudan University, Shanghai, China

*Corresponding author. Tel: +86 21 54237304; E-mail: fxyu@fudan.edu.cn

The Hippo signaling pathway plays a critical role in early development, tissue regeneration, and tumorigenesis [16–19]. The physiological and pathological functions of the Hippo pathway are largely mediated by two homologous transcriptional co-activators, YAP and TAZ. When the Hippo pathway is on, YAP and TAZ are phosphorylated by upstream kinases LATS1/2, leading to their cytoplasmic retention. Conversely, when Hippo signaling is off, dephosphorylated YAP and TAZ translocate into nucleus, interact with TEAD family transcription factors, and induce the expression of target genes. YAP and TAZ target genes promote cell proliferation, survival, migration, and epithelial–mesenchymal transition (EMT), which together leads to organ growth and tumorigenesis.

Recently, novel functions of YAP/TAZ in immune system have been uncovered. In the *Drosophila* immune organ fat bodies, Yorkie (Yki, a YAP ortholog) activity is repressed by Gram-positive bacteria, which leads to lower production of antimicrobial peptides [20]. In mammals, by interacting with TBK1 or IRF3, YAP/TAZ inhibits production of type I IFNs [21,22]. Moreover, it has been revealed recently that TAZ is required for the differentiation of pro-inflammatory T_H17 cells, whereas YAP is involved in maintaining immunosuppressive regulatory T (Treg) cells [23,24]. Together, these evidences demonstrate that YAP/TAZ activity regulates both innate immunity and adaptive immunity.

In this study, we identified a novel TAZ isoform called cTAZ that was transcribed by an alternative promoter. cTAZ contains the majority of the C-terminus sequence of TAZ, but not the TEAD-binding domain (TBD) and WW domain, and thus lacks canonical Hippo pathway functions. Type I IFN-triggered JAK-STAT signaling directly induces the expression of cTAZ, and cTAZ in turn inhibits JAK-STAT signaling by disrupting the dimerization and nuclear translocation of STAT1 and STAT2, thereby down-regulating the expression of ISGs and cellular antiviral response. Thus, cTAZ serves as a modulator to restrain type I IFN responses following viral infections.

Results and Discussion

A short TAZ isoform, cTAZ, is transcribed by an alternative promoter

We used anti-YAP/TAZ and anti-TAZ (CST) antibodies targeting the C-terminus of TAZ to determine the expression of YAP/TAZ across different cell lines (Fig 1A). In immunoblotting (IB), these C-terminus-specific antibodies detected YAP (~70 kDa), TAZ

(~55 kDa), and unexpectedly a smaller protein (~37 kDa, as indicated by an asterisk; Fig 1B). The small protein was encoded by the TAZ gene as its expression was reduced by treating cells with shRNA targeting TAZ but not YAP (Fig 1C). In an immunoprecipitation (IP) assay, this smaller protein was immunoprecipitated and recognized by anti-TAZ (CST) or anti-YAP/TAZ antibody, but failed to be immunoprecipitated or react with anti-TAZ (SA), an antibody targeting the N-terminus of TAZ (aa36–175; Figs 1A and D, and EV1A and B). These results suggested that the ~37-kDa protein is a shorter TAZ isoform comprising mainly the C-terminal TAZ sequence; thus, it was dubbed as cTAZ (C-terminus of TAZ). cTAZ protein was detected in about 30% of the cell lines tested in this study (Appendix Table S1), and cTAZ mRNA was detected in most human tissues, albeit at low levels (Appendix Table S2). In mouse tissues, we failed to detect cTAZ protein expression in organs like liver and heart, whereas a band at the molecular weight of cTAZ was detected in lymph nodes and thymus (Fig EV1C). Moreover, mRNA and protein expression of cTAZ was detected in surgically removed lymph nodes of ~50% thyroid cancer patients (Fig EV1D).

To determine whether cTAZ was generated by proteolytic cleavage of full-length TAZ or encoded by an alternative transcript, we overexpressed a C-terminal HA-tagged YAP or TAZ in RKO or Caco2 cell. A band corresponding to cTAZ was not detected following overexpression (Figs 1E and EV1E), indicating that cTAZ was unlikely to be generated through proteolysis. We then analyzed RNA-seq data of HCT-116 cells (which also expresses cTAZ, Appendix Table S1) from Sequence Read Archive (SRA) database and spotted a short TAZ transcript (ENST00000472417) comprising a novel 5'UTR, an alternative exon, and exons encoding the C-terminal sequence of conventional TAZ (Fig 1F). PCR with primers targeting this novel 5'UTR from cDNA of RKO cells expressing cTAZ, but not HEK293A cells that did not express cTAZ, yielded products of the expected band size (Fig 1F and G). The PCR product was identical in sequence to the variant available in the SRA database, it included amino acids 145–400 of full-length TAZ and two novel amino acids (extreme N-terminal) encoded by the alternative exon (Fig 1H). These results suggested that cTAZ was encoded by a transcription variant. Using CRISPR/Cas9 technology, we were able to ablate cTAZ from RKO cells by targeting cTAZ-specific 5'UTR region (Figs 1I, and EV1F and G).

We further sought to ascertain whether the cTAZ mRNA was generated by alternative splicing or transcribed by an alternative promoter. By comparing the mRNA levels of cTAZ and TAZ in various human tissues using RNA-seq data from Genotype-Tissue

Figure 1. Identification of a short TAZ isoform transcribed by an alternative promoter.

- YAP and/or TAZ antibodies and their target regions.
- Expression of YAP/TAZ and a smaller protein (asterisk) in different cell lines, protein expression was determined by immunoblotting (IB).
- The shRNA targeting TAZ, but not YAP, knocked down the expression of the smaller protein (asterisk).
- Antibodies targeting C-terminus YAP/TAZ, such as TAZ (CST) and YAP/TAZ, effectively pulled down the smaller protein (asterisk, dubbed as cTAZ hereafter) in RKO cells in an immunoprecipitation (IP) assay. cTAZ was not recognized by TAZ (SA), an antibody targeting N-terminus of TAZ.
- Exogenous TAZ/YAP was not processed proteolytically to cTAZ. RKO cells were transfected with the indicated plasmids expressing C-terminal HA-tagged TAZ or YAP.
- UCSC Genome Browser view of TAZ isoforms. Displayed tracks include a short (cTAZ?) and the full-length (TAZ) transcript of TAZ assembled using RNA-seq data of HCT-116 cells from SRA. The short TAZ isoform was similar to transcript ENST00000472417 annotated in Ensembl database. Below: the H3K9ac, H3K27ac, H3K4me1, H3K4me2, and H3K4me3 histone-modification signal peaks across TAZ gene in HCT-116 cells (data from ENCODE database). The red arrows indicate the primers (F: forward; R: reverse) used in (G). UTR and exons are shown in green blocks.
- RKO, but not HEK293A cells, expressed both full-length TAZ and cTAZ transcripts. RT–PCR primers targeting different regions are shown in (F).
- Alignment of TAZ and cTAZ protein sequences. cTAZ protein sequence was derived from the Sanger sequencing results of the short PCR product (RKO, F2:R1) in (G).
- Knockout of cTAZ in RKO cells using CRISPR/Cas9 technology. Monoclonal (#3 and #14) were selected.

Source data are available online for this figure.

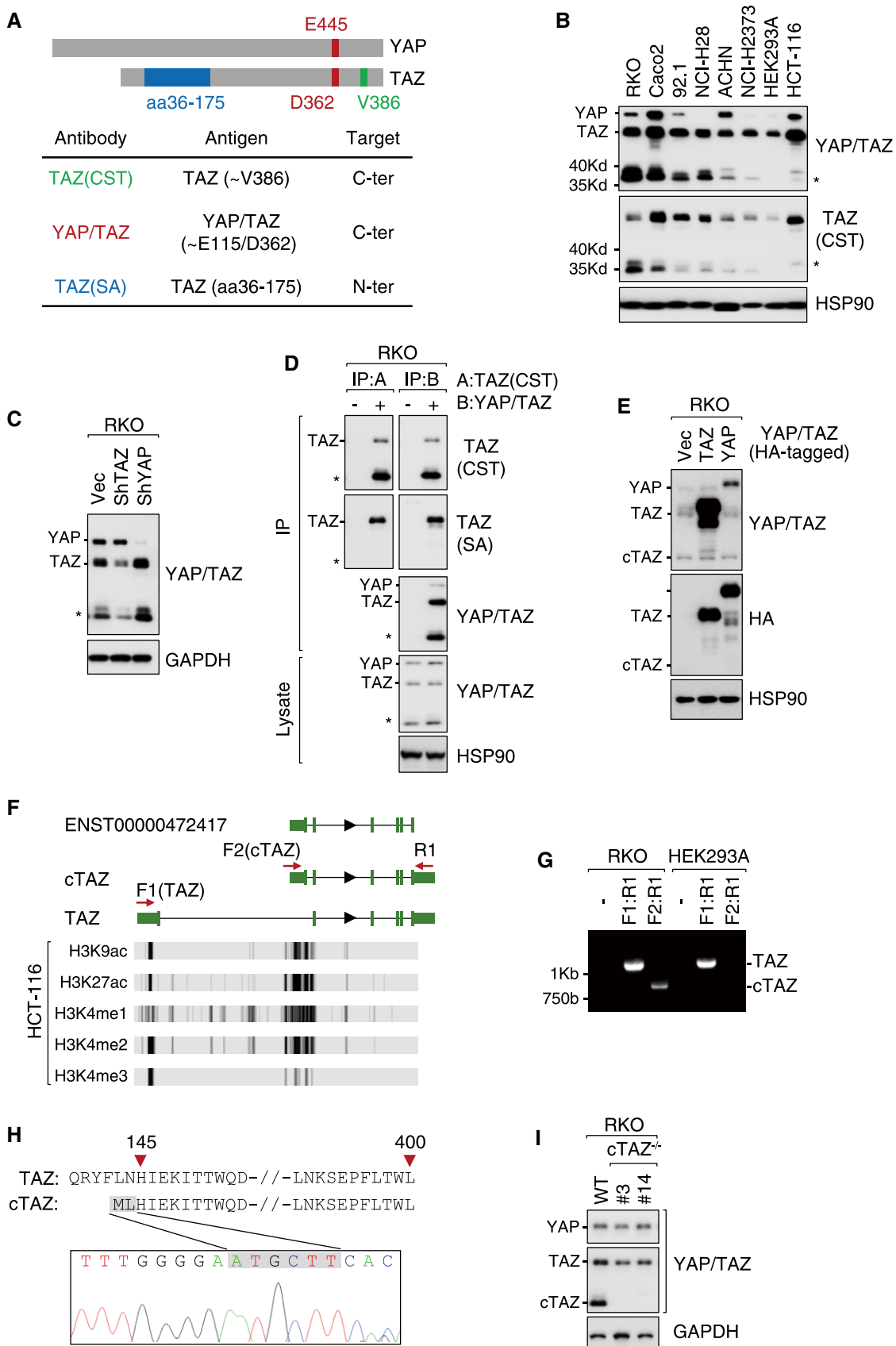


Figure 1.

Expression database, we found no association (Fig EV1H). At the protein level, expression levels of cTAZ and TAZ were also not correlated in diverse cell lines (Fig 1B). Moreover, the region around cTAZ 5'UTR harbors a typical promoter sequence with a predicted TATA box and was intensively marked by active epigenetic modifications such as H3K9ac, H3K27ac, H3K4me1, H3K4me2, and H3K4me3 (Fig 1F, and Appendix Fig S1). On the other hand, active epigenetic modifications were not present near cTAZ 5'UTR in MCF-7 cells, a cell line without cTAZ expression (Fig EV1I, Appendix Table S1). These evidences collectively suggest that cTAZ was transcribed by an alternative promoter.

cTAZ is not regulated by Hippo signaling

The interaction between YAP/TAZ and their upstream kinases LATS1/2 is mediated by WW domains in YAP/TAZ and PPxY motifs in LATS1/2 [25]. cTAZ lacks an intact WW domain (Fig EV2A), suggesting that it cannot interact with LATS1/2 or respond to upstream signals. In a co-immunoprecipitation (Co-IP) assay, wild-type YAP and TAZ efficiently pulled down endogenous LATS2, whereas cTAZ or WW-mutated YAP/TAZ (YAP WW1/2 or TAZ WW) failed to precipitate LATS2 (Fig EV2B). Thus, cTAZ was unlikely affected by LATS1/2 kinase activity.

The Hippo pathway senses many environmental cues, such as cell-cell contact, matrix stiffness, and diffusible ligands for G-protein-coupled receptors (GPCR) [25–27]. YAP/TAZ phosphorylation by LATS1/2 leads to subsequent ubiquitination and degradation of YAP/TAZ [28]. Notably, serum starvation controls the phosphorylation and protein levels of YAP/TAZ (S61, S109, S127, S164, and S381 of YAP, and S66, S89, S117, and S311 of TAZ) in a LATS1/2-dependent manner [28,29]. Both endogenous and exogenous full-length TAZ exhibited a significant increase in phosphorylation (as indicated by an upshift in regular or Phostag gel electrophoresis, or blotting using a YAP S127 phosphorylation-specific antibody), whereas cTAZ was not regulated by serum starvation (Fig EV2C and D). Indeed, when cells were treated with cycloheximide (CHX), an inhibitor of protein synthesis, the half-life of cTAZ protein was longer than that of full-length TAZ (Fig EV2E and F). Moreover, half-life of full-length TAZ but not cTAZ was stabilized in *LATS1/2*-double-knockout cells or under serum-rich conditions (Fig EV2E and F). Taken together, these results suggest that cTAZ was not regulated by LATS1/2 or upstream signals.

cTAZ lacks TEAD-mediated transcriptional activity and canonical TAZ functions

The biological functions of YAP/TAZ are mainly mediated by TEAD family transcription factors, and TEAD-binding domains (TBD) are mapped to the N-terminus of YAP/TAZ (Fig EV2A). The entire TBD is absent in cTAZ; thus, cTAZ is not expected to induce TEAD-mediated transcription and canonical Hippo pathway functions. Indeed, cTAZ could not interact with TEAD proteins as TAZ did (Fig EV3A). In a luciferase assay, the activity of an 8×GTTC reporter, which reflects TEAD-mediated transcriptional activity, was up-regulated by full-length TAZ, but unaffected by cTAZ (Fig EV3B). Moreover, expression of *CTGF* and *CYR61*, two TEAD-mediated YAP/TAZ target genes, was significantly induced by full-length TAZ, but not by cTAZ (Fig EV3B–D). Together, these results indicate that cTAZ lacks TEAD-mediated transcriptional activity.

As oncoproteins, YAP/TAZ can promote cell proliferation, migration, EMT, and transformation [29–31]. However, overexpression of cTAZ failed to down-regulate E-cadherin or up-regulate N-cadherin and vimentin, which are hallmarks of EMT (Fig EV3D). In addition, overexpression of full-length TAZ but not cTAZ induced cellular morphological changes, F-actin reorganization, and anchorage-independent growth of MCF-10A cells (Fig EV3E and F). Moreover, in lung squamous cell carcinoma (LUSC), high expression of TAZ could predict a poor patient survival, whereas cTAZ expression was not associated with prognosis (Fig EV3G). These evidences suggest that cTAZ does not possess the canonical growth-promoting and oncogenic activities of TAZ.

cTAZ directly suppresses JAK-STAT signaling

To further characterize the function of cTAZ, we performed RNA-seq in wild-type, *cTAZ*-knockout (*cTAZ*^{-/-}), and *cTAZ*-complemented (*cTAZ*^{-/-} GFP-cTAZ) cells. We identified 103 differentially expressed genes, which were affected by cTAZ deficiency and rescued by GFP-cTAZ complementation (Figs 2A and EV4A, Dataset EV1). Gene ontology (GO) analysis indicated that these differentially expressed genes were mainly enriched in type I IFN signaling, defense response to virus, and immune system process (Fig 2B), with many being well-defined ISGs [32,33]. Some cTAZ-targeted genes, such as *DDX58*, *IRF7*, *IFIH1*, *STAT1*, *OAS1*, *MX1*, and *IRF9*, were assessed by qPCR in multiple *cTAZ*^{-/-} clones (Fig 2C). The protein levels of RIG-I (encoded by *DDX58*), IRF9, and MX1 in *cTAZ*-knockout cells were also elevated, whereas IRF7 and STAT1 protein levels were not significantly changed upon *cTAZ* ablation (Fig EV4B). Thus, expression of an array of ISGs was repressed by cTAZ.

Type I IFNs activate JAK-STAT signaling and promote ISG expression [34,35]. We then tested whether cTAZ could regulate the expression of ISGs induced by JAK-STAT signaling. cTAZ expression dramatically repressed the activity of an ISRE reporter induced by IFN- α (Fig 2D). cTAZ-mediated repression of the ISRE reporter was similarly observed in cells treated with condition medium containing type I IFNs from cells expressing constitutively active RIG-I (caRIG-I, aa1–284 of RIG-I [22,36]; Fig EV4C).

YAP/TAZ can block IRF3 activation and inhibit type I IFNs production [21,22]. IRF7 is a target gene of STAT1/2 and can also induce IFN production; thus, IRF3 and IRF7 may interfere the assay by regulating IFN levels. We generated *IRF3/7*-double-knockout (dKO) cells, which were significantly less competent to caRIG-I in activating the ISRE reporter (Fig EV4D and E). However, the response of *IRF3/7* dKO cells to IFN- α was identical to that of wild-type cells (Figs 2D and EV4F). More importantly, under IFN- α stimulation, the expression of ISGs, such as *IFIH1* and *STAT1*, was super-induced when cTAZ was ablated (Fig 2E). In addition, the mRNA levels of IFNB in RKO cells were not significantly repressed when cTAZ was overexpressed (Fig EV4G). Taken together, these results suggest that, rather than modulating the production of IFNs, cTAZ can regulate the robustness of JAK-STAT signaling directly.

cTAZ inhibits dimerization and nuclear translocation of phosphorylated STAT1/2

We next investigated the molecular mechanism by which cTAZ regulates JAK-STAT signaling. Upon IFN stimulation, phosphorylation of

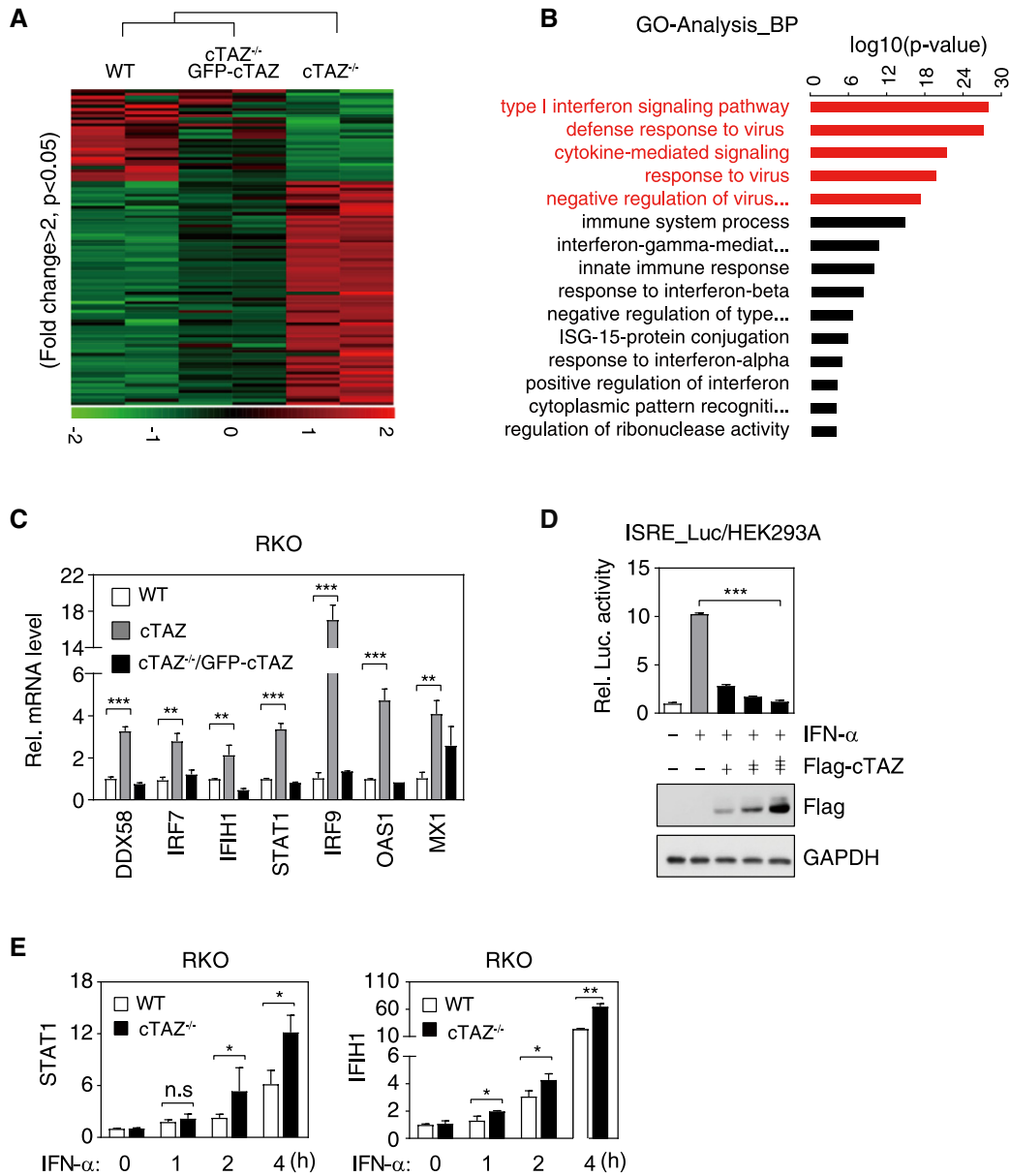


Figure 2. cTAZ directly represses JAK-STAT signaling.

A Cluster analysis of RNA expression of WT, cTAZ^{-/-}, and cTAZ^{-/-}/GFP-cTAZ put-back RKO cells. Genes down- and up-regulated more than twofold ($P < 0.05$) in cTAZ KO cells were included in cluster analysis. Green and red indicate down- and up-regulated genes, respectively.

B Gene ontology (GO) analysis identified differentially regulated pathway by cTAZ.

C cTAZ suppressed expression of ISGs. RNA levels of selected ISGs in WT, cTAZ^{-/-}, and cTAZ^{-/-}/GFP-cTAZ RKO cells were quantified by qPCR. Error bars indicate SD, $n = 3$. ** $P < 0.01$; *** $P < 0.001$; Student's t -test.

D cTAZ repressed 5xISRE-luciferase activity induced by IFN- α . HEK293A cells were transfected with 5xISRE-luciferase reporter along with the indicated plasmids, treated with or without IFN- α (50 ng/ml) for 12 h. The expression of ectopic gene was determined by IB. Error bars indicate SD, $n = 3$. *** $P < 0.001$; one-way ANOVA test was used for statistical analysis.

E Knockout of cTAZ promoted ISG expression in the presence of IFN- α . WT and cTAZ^{-/-} RKO cells were treated with or without of IFN- α (50 ng/ml) for indicated time, and expression of selected genes was quantified by qPCR. WT or cTAZ^{-/-} group was normalized by basal level, respectively. Error bars indicate SD, $n = 3$. * $P < 0.05$; ** $P < 0.01$; Student's t -test.

Source data are available online for this figure.

STAT proteins (such as tyrosine 701 (Y701) of STAT1) by JAK kinases serves as a molecular switch to activate the pathway [37,38]. In wild-type and cTAZ^{-/-} RKO cells, no difference in Y701

phosphorylation of STAT1 protein was observed following IFN- α treatment (Fig EV5A). Moreover, ectopic cTAZ failed to block the phosphorylation of other sites of STAT proteins (such as Y705 of

STAT1 and Y694 of STAT5) induced by IFN- α in HEK293A cells (Fig EV5B). Thus, cTAZ does not regulate STAT phosphorylation by their upstream kinases.

We then used the proximity-dependent biotin identification (BioID) to interrogate the potential interactions between cTAZ and

components of the JAK-STAT pathway (Fig EV5C). The only hit of this screen was STAT1 (Fig EV5D and Dataset EV2). In a Co-IP assay, ectopic cTAZ interacted with STAT1, and the interaction is increased upon IFN- α treatment (Fig 3A). Following extensive mapping experiments, we found that amino acids 59–87 of cTAZ

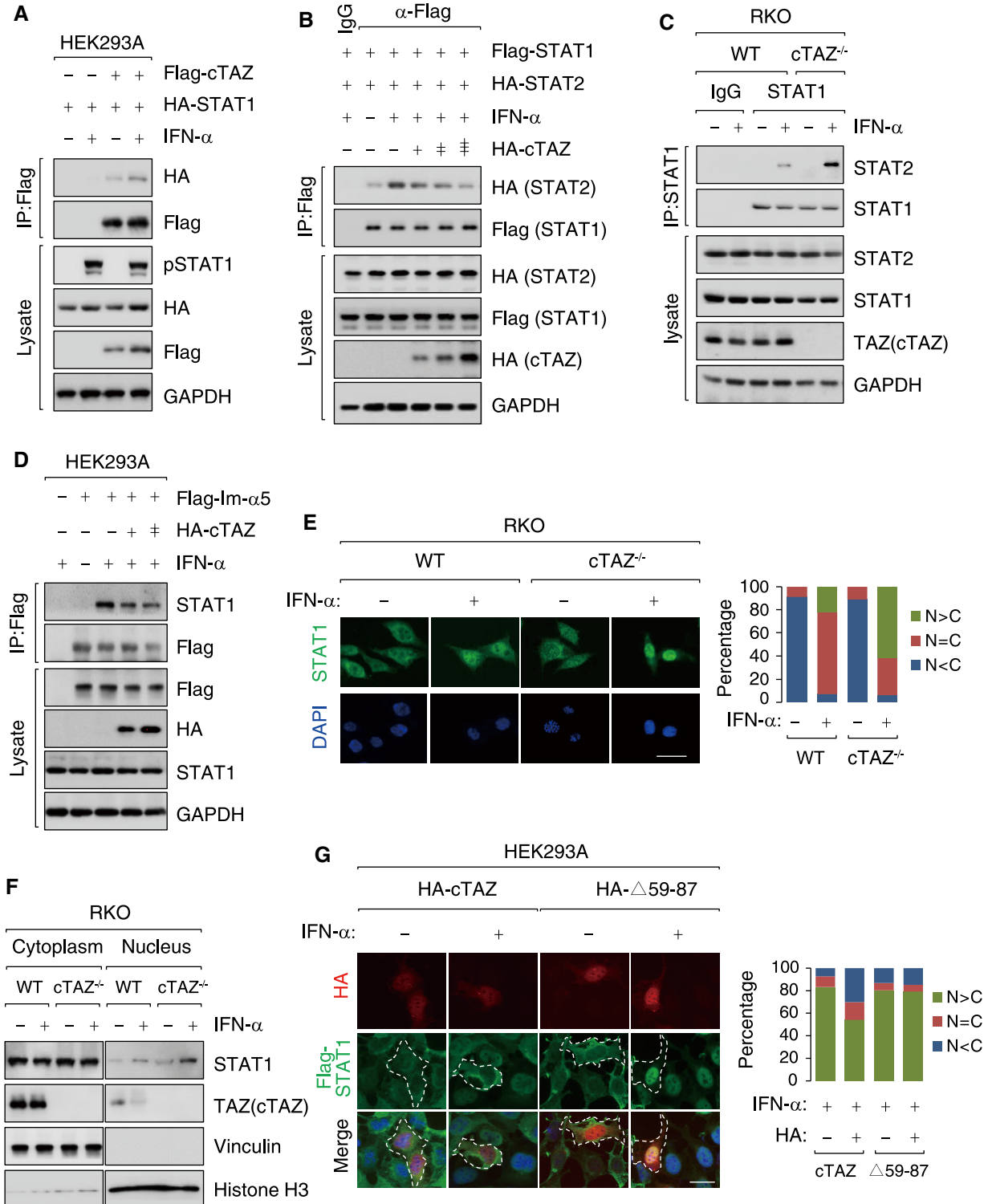


Figure 3.

Figure 3. cTAZ attenuates dimerization and nuclear translocation of STAT1/2.

- A STAT1 interacted with cTAZ, and the interaction was enhanced by IFN- α . HEK293A cells were transfected with indicated plasmids, treated with or without IFN- α (50 ng/ml) for 1 h. IP were performed using Flag antibody.
- B cTAZ attenuated heterodimerization between STAT1 and STAT2 induced by IFN- α . Following transfection, cells were treated with or without IFN- α (50 ng/ml) for 1 h and subjected to IP assays using Flag antibody.
- C Depletion of cTAZ enhanced the interaction between STAT1 and STAT2. RKO cell lines (WT and #14) were treated with IFN- α as in (B). IP assays were performed using STAT1 antibody.
- D cTAZ attenuated interaction between STAT1 and importin- α 5 (Im- α 5). Following transfection, HEK293A cells were stimulated using IFN- α as in Fig 2B. IP assays were performed using Flag antibody.
- E Deletion of cTAZ promoted nuclear accumulation of STAT1 upon IFN- α stimulation. RKO (WT and cTAZ^{-/-}) cells treated with or without IFN- α (50 ng/ml) for 1 h, fixed, and subjected to IF using STAT1 antibody (green). DNA was labeled by DAPI (blue). Scale bar, 50 μ m. Quantification was performed using ImageJ software (right). N>C: nuclear; N = C: nuclear plus cytoplasmic; N<C: cytoplasmic localization.
- F Deletion of cTAZ promoted nuclear accumulation of STAT1 upon IFN- α stimulation. Cells were treated as in (E) and subjected to subcellular fractionation.
- G cTAZ defective in STAT1-binding failed to block nuclear translocation of STAT1. HEK293A stably overexpressing STAT1 were transfected with the indicated plasmids, treated with or without IFN- α (50 ng/ml) for 1 h, fixed, and subjected to IF as in (E). Scale bar, 25 μ m.

Source data are available online for this figure.

and the SH2 domain of STAT1 were essential for cTAZ-STAT1 interaction (Fig EV5E and F). The SH2 domain of STAT1/2 was critical for their homo- or heterodimerization [39]. We speculated that cTAZ may perturb the interaction between STAT1 and STAT2. Indeed, ectopic cTAZ, but not amino acids 59–87-deleted cTAZ (cTAZ Δ 59–87), abrogated STAT1/2 dimerization induced by IFN- α (Figs 3B and EV5G). Moreover, knockout of endogenous cTAZ could promote STAT1/2 interaction stimulated by IFN- α in RKO (Fig 3C).

The dimerization of phosphorylated STAT1/2 is essential for interaction with importin- α 5 and nuclear translocation [37,38,40,41]. We found that ectopic cTAZ, but not cTAZ Δ 59–87, attenuated the interaction between STAT1 and importin- α 5 in a dose-dependent manner (Figs 3D and EV5H). In an IF assay, about 30% of WT cells and 50–60% of cTAZ^{-/-} cells, respectively, showed strong nuclear STAT1/2 localization following IFN- α stimulation (Figs 3E and EV5I). Nuclear enrichment of STAT1 in cTAZ-knockout cells was also observed in a cell fractionation assay (Fig 3F). Moreover, overexpression of cTAZ, but not cTAZ Δ 59–87, blocked STAT1 nuclear entry upon IFN- α treatment (Fig 3G). Taken

together, cTAZ attenuates JAK-STAT signaling by disrupting the dimerization of phosphorylated STAT1/2 and blocking their nuclear translocation.

cTAZ negatively regulates cellular antiviral response

A major function of type I IFN-induced JAK-STAT signaling is to limit viral infection [15]. We subsequently tested whether cTAZ could regulate antiviral response. In HEK293A or HCT-116 cells, overexpression of STAT1/2 efficiently blocked the replication of GFP-labeled vesicular stomatitis virus (gVSV, an RNA virus), and cTAZ overexpression abolished the antiviral effect of STAT1/2 without affecting STAT1/2 expression (Fig 4A and B, and Appendix Fig S2A and B). Similar results were obtained using GFP-labeled herpes simplex virus (gHSV, a DNA virus; Appendix Fig S2C). In contrast, cTAZ Δ 59–87, which was defective in binding to STAT1/2, failed to repress the antiviral effect of STAT1/2 (Appendix Fig S2D). We also found that ectopic expression of cTAZ could neutralize the antiviral activity of IFN- α in a dose-dependent manner (Fig 4C). To prove JAK-STAT signaling pathway is required for the inhibitory function

Figure 4. cTAZ negatively regulates cellular antiviral response.

- A cTAZ repressed the antiviral activity of ectopic STAT1/2. HEK293A cells were transfected with indicated plasmids, infected with gVSV (MOI = 0.01) for 12 h, fixed, and subjected to microscopy (Left). Viral infection and replication were marked by green fluorescence. Scale bar, 100 μ m. (Right) Quantification of GFP-positive cells. About 300 cells (from three different fields) were analyzed. Error bars indicate SD. ** P < 0.01; *** P < 0.001; Student's t -test.
- B cTAZ and STAT1/2 expression levels of cells used in (A).
- C cTAZ effectively repressed antiviral activity of IFN- α . Transfection and infection were performed as in (A). Top: GFP intensity of cell lysates was measured by a fluorometer. Bottom: Viral GFP and ectopic cTAZ protein levels were detected by IB.
- D Depletion of cTAZ repressed viral replication. RKO cell lines (WT and two independent cTAZ^{-/-} clones) were infected with gVSV (MOI = 0.1) for 12 h. Scale bar, 100 μ m. The ratio of GFP-positive cells were calculated as in (A). About 300 cells (from three different fields) were analyzed. Error bars indicate SD. *** P < 0.001; Student's t -test.
- E Depletion of cTAZ repressed viral replication. Cells were treated as in (D), and GFP intensity of cell lysates was measured. Error bars indicate SD, n = 3. ** P < 0.01; *** P < 0.001; Student's t -test.
- F Depletion of cTAZ repressed viral replication. Cells were treated as in (D), and the viral genomic RNA was quantified by qPCR (normalized to human GAPDH). Error bars indicate SD, n = 3. *** P < 0.001; Student's t -test.
- G cTAZ deficiency enhanced ISG expression. Cells were treated as in (E), and expression of *IFIH1* and *DDX58* was assessed by qPCR. Error bars indicate SD, n = 3. * P < 0.05; ** P < 0.01; *** P < 0.001; Student's t -test.
- H Overexpression of cTAZ promotes virus infection. DOX-inducible cTAZ-overexpressing RKO cell lines were pre-treated with DOX for 48 h (1 μ g/ml). gVSV infection and GFP fluorescence intensity quantification were performed as in (D). Error bars indicate SD, n = 3. ** P < 0.01; *** P < 0.001; Student's t -test.
- I Overexpression of cTAZ repressed ISG expression. Cells were treated as in (H), and expression of *IFIH1* and *DDX58* was assessed by qPCR. Error bars indicate SD, n = 3. * P < 0.05; ** P < 0.01; Student's t -test.

Source data are available online for this figure.

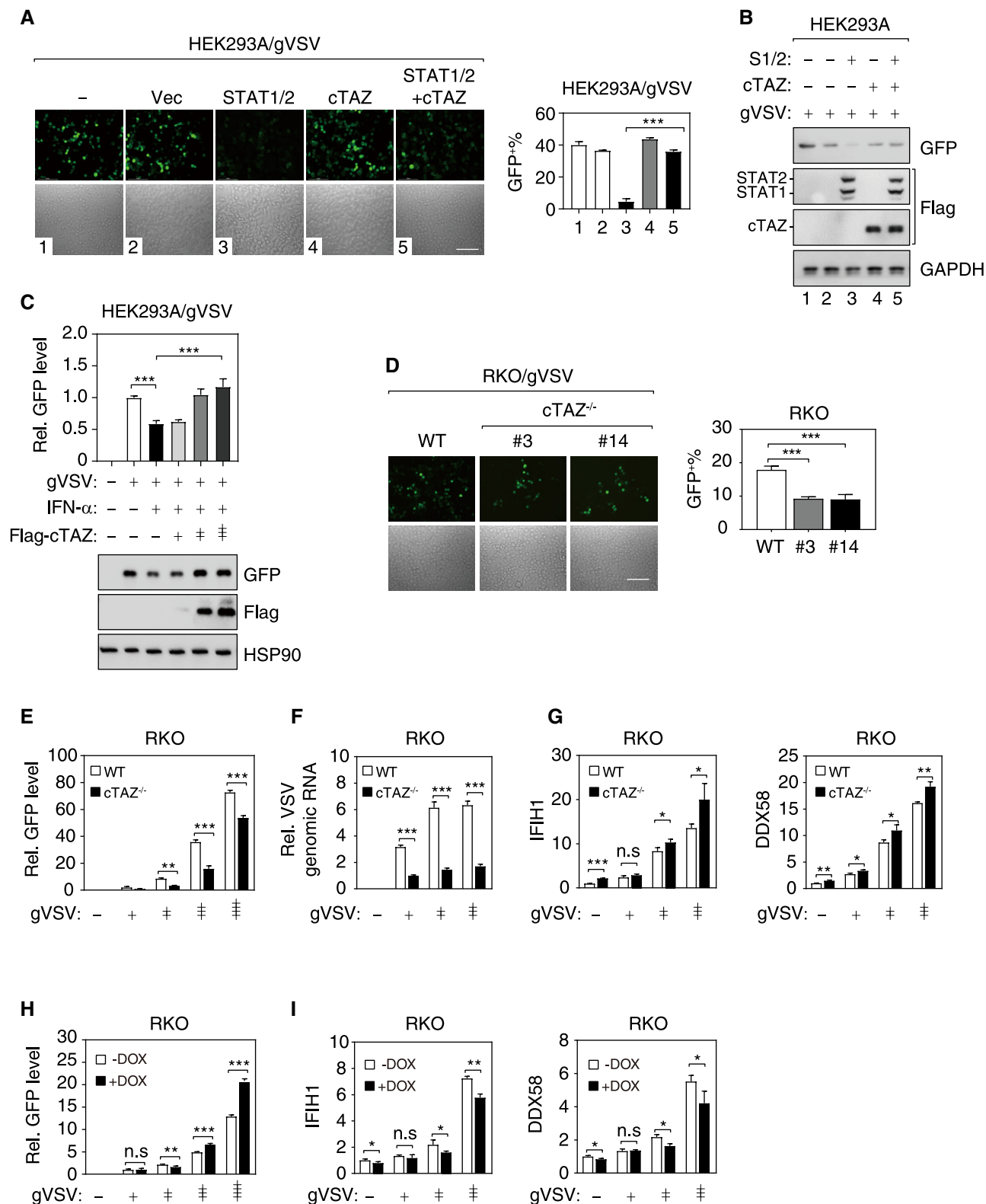


Figure 4.

of cTAZ in cellular antiviral activity, we generated *JAK1*-knockout cells (Appendix Fig S2E), and in these cells, ectopic cTAZ could not repress viral replication (Appendix Fig S2F).

We further investigated the inhibitory function of endogenous cTAZ in cellular antiviral activity. In *cTAZ*^{-/-} RKO cells, the replication of gVSV and gHSV was significantly inhibited, as indicated by

fewer GFP-positive cells, lower intensity of GFP fluorescence, and/or lower viral genome copy number (Fig 4D–F, and Appendix Fig S2G and H). Meanwhile, the expression of ISGs was significantly increased in *cTAZ*^{-/-} RKO following viral infection (gHSV and gVSV) (Fig 4G and Appendix Fig S2I).

We also established doxycycline (DOX)-inducible *cTAZ*-expressing cells, and observed that inducible *cTAZ* expression enhanced the replication of virus (gVSV and gHSV) and attenuated ISG expression (Fig 4H and I, and Appendix Fig S2J–L). Together, *cTAZ* negatively regulates cellular antiviral response by inhibiting JAK-STAT signaling and expression of ISGs.

***cTAZ* regulates antiviral response in a Hippo signaling-independent manner**

The major difference between *cTAZ* and full-length TAZ and YAP was their response to Hippo pathway kinases and upstream signals. Full-length TAZ and YAP also interacted with STAT1 as shown in the BioID experiment (Fig EV5D), and they also had the motif (aa59–87 in *cTAZ*) responsible for STAT1 binding. We therefore tested the effect of full-length TAZ and YAP on JAK-STAT signaling and cellular antiviral response. In a Co-IP assay, full-length TAZ and YAP could interact with STAT1 (Appendix Fig S3A), indicating that full-length TAZ and YAP could negatively regulate JAK-STAT signaling, in a similar fashion as *cTAZ* did.

We also tested the effect of *cTAZ* and full-length TAZ and YAP on the expression of ISGs and ISRE promoter activities under different cell densities and serum concentrations, two robust upstream signals of the Hippo pathway [25,27]. Interestingly, under low cell density or serum-rich conditions, the effect of *cTAZ* and full-length TAZ and YAP on the expression of ISGs and ISRE promoter activity was indistinguishable; however, under high cell density and serum starvation conditions, *cTAZ* remained effective whereas full-length TAZ and YAP were unable to repress ISG expression or ISRE promoter activity (Appendix Fig S3B and C). Moreover, the interaction between full-length TAZ and STAT1 was reduced under serum starvation, whereas *cTAZ* and STAT1 interaction was not sensitive to serum (Appendix Fig S3D). The effect of full-length YAP toward ISG expression in a Hippo signaling-dependent manner was

consistent with a previous report [22]. These results suggested that, compared to full-length TAZ and YAP, *cTAZ* could regulate antiviral response under diverse conditions in a Hippo signaling-independent manner.

In 2017, two groups reported a role of YAP (and TAZ) in antiviral response [21,22]. Zhang *et al* [22] demonstrated that YAP prevented TBK1 binding to STING/MAVS and blocked virus-induced TBK1 activation. Wang *et al* [21] reported that YAP, independent of its transcriptional activity, blocked the dimerization of the transcription factor IRF3 to impede nuclear translocation following viral infection. Although different mechanisms were proposed, both studies reached a same conclusion that YAP blocked virus-induced production of type I IFNs and impaired host antiviral response. Our results indicate that *cTAZ* also represses antiviral response, but not by limiting type I IFN production and instead by inhibiting JAK-STAT signaling. Furthermore, both full-length TAZ and YAP could interact with STAT1 and limit antiviral response in sparse culture and serum-rich conditions; on the other hand, the effect of *cTAZ* was independent on Hippo signaling (Appendix Fig S3). We propose that, *cTAZ* and full-length TAZ and YAP may limit antiviral response via multiple mechanisms, including the production and downstream signaling of type I IFNs. Moreover, compare to full-length TAZ and YAP, *cTAZ* may regulate antiviral response under broader situations.

As oncoproteins, YAP/TAZ can profoundly promote cell proliferation and inhibit cell differentiation. Should the expression and activity of YAP/TAZ be regulated by type I IFNs, the fate of the responding cells may undergo dramatic change upon infection. Conceivably, *cTAZ* does not participate in the canonical Hippo pathway, and can function as a specialized regulator for the JAK-STAT signaling pathway during antiviral response.

***cTAZ* expression is induced by JAK-STAT signaling**

The IFN response mediated by the JAK-STAT signaling pathway is tightly controlled by negative regulators, such as *SOC1* and *USP18* [5,42,43]. We noticed that gVSV infection induced expression of *cTAZ* protein (Fig 5A), indicating *cTAZ* as a target gene of JAK-STAT signaling. When cells were treated with IFN- α , both

Figure 5. *cTAZ* expression was induced by JAK-STAT signaling.

- gVSV induced expression of *cTAZ*. RKO cells were infected with gVSV (MOI = 0, 0.001, 0.01, 0.01, 1) for 8 h. Protein expression was determined by IB (Left) and quantified (Right). Error bars indicate SD, $n = 3$. *** $P < 0.001$; two-way ANOVA test was used for statistical analysis.
- IFN- α induced expression of *cTAZ*. RKO cells were treated with different doses of IFN- α for 8 h. Protein expression was determined as in (A). Error bars indicate SD, $n = 3$. *** $P < 0.001$; two-way ANOVA test was used for statistical analysis.
- IFN- α induced mRNA level of *cTAZ*. RKO cells were treated with different doses of IFN- α for 8 h. RNA levels were measured by qPCR. Error bars indicate SD, $n = 3$. *** $P < 0.001$; two-way ANOVA test was used for statistical analysis.
- STAT1/2 synergistically activated a *cTAZ* promoter. HEK293A cells were transfected with *cTAZ* reporter with or without STAT proteins. Promoter activity was determined using luciferase assay, and protein expression was determined by IB. Error bars indicate SD, $n = 3$. *** $P < 0.001$; Student's *t*-test.
- STAT1/2 binding sites on *cTAZ* promoter. HEK293A cells were transfected with *cTAZ* promoters (wild type or mutants). Luciferase activity and responses to STAT1/2 expression were measured. Error bars indicate SD, $n = 3$. ** $P < 0.01$; Student's *t*-test.
- STAT1 occupied *cTAZ* promoter in an IFN- α -sensitive manner. RKO cells were treated with or without IFN- α (50 ng/ml) for 1 h and subjected to CHIP assays. *cTAZ* PCR primers were designed to target STAT1/2 binding site. ISG15 promoter was included as a positive control.
- A negative feedback mechanism regulating JAK-STAT signaling involving *cTAZ*. Upon IFN- α stimulation, STAT1/2 are phosphorylated and undergo dimerization. STAT1/2 dimer interacts with importins (such as Im- α 5), enters nucleus, and activates transcription of target genes including ISGs. The expression of *cTAZ* is induced by STAT1/2. Elevated *cTAZ* blocks the dimerization and nuclear translocation of STAT1/2, which in turn leads to repression of the JAK-STAT signaling. *cTAZ* represents a critical node of a negative feedback mechanism regulating the JAK-STAT signaling.

Source data are available online for this figure.

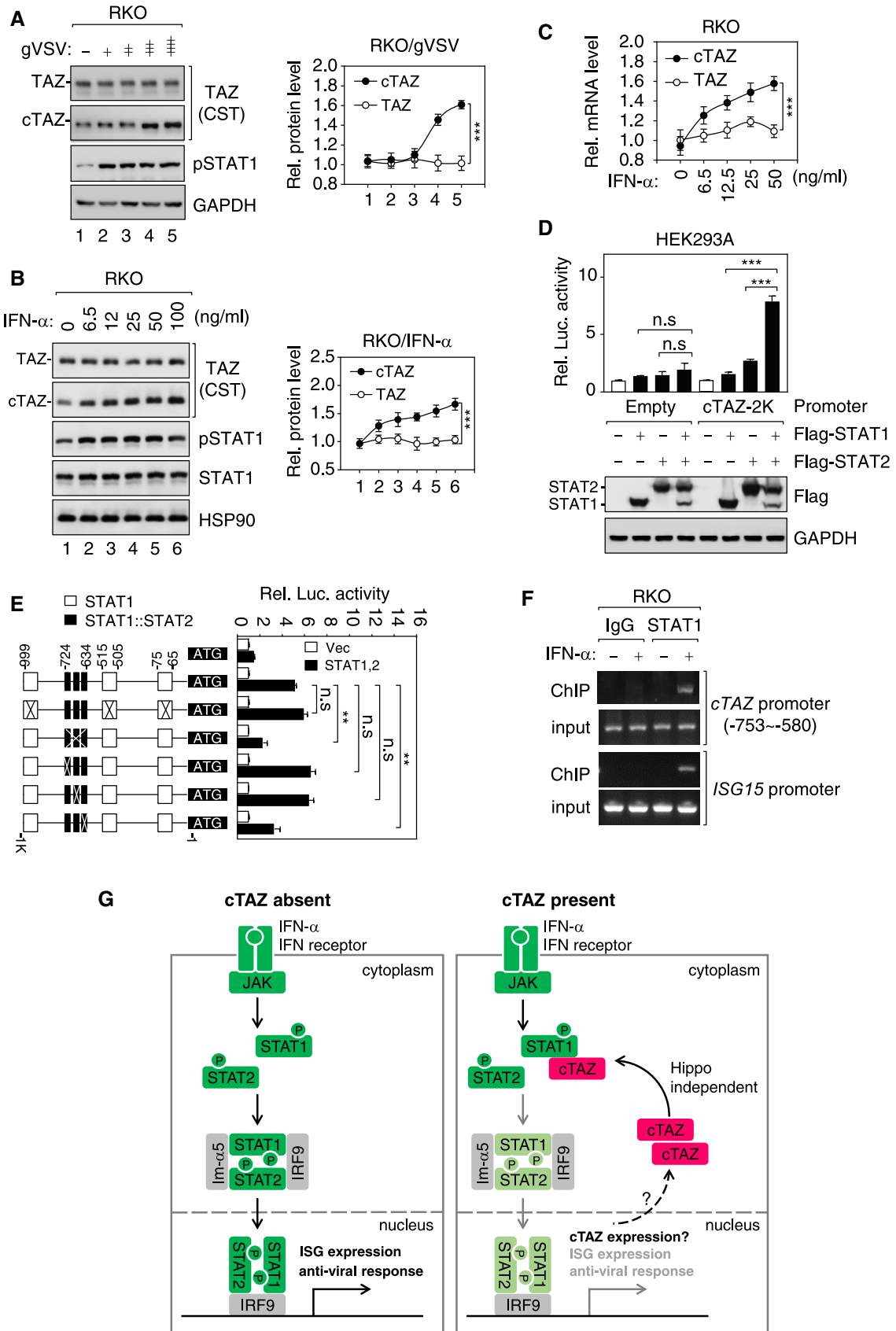


Figure 5.

cTAZ transcript and protein were induced in a dose-dependent manner; in contrast, *TAZ* was not regulated by $\text{IFN-}\alpha$ (Fig 5B and C, and Appendix Fig S4A and B). Moreover, a luciferase reporter of *cTAZ* promoter activity (~2,000 bp upstream of the translation starting site) was activated by ectopic *caRIG-I* or *STAT1/2* (Fig 5D and Appendix Fig S4C), and a shorter promoter (~1,000 bp upstream of the translation starting site) similarly responded to overexpression of *caRIG-I* or *STAT* proteins (Appendix Fig S4C and D). Using the JASPAR software, we identified three *STAT1* (–999, –515, and –75) and three *STAT1/2* (–724, –666, and –648) binding sites in the *cTAZ* promoter (Fig 5E). Subsequent mutagenesis experiments revealed that three *STAT1/2*-binding sites, especially the one near –634 position, were required for *STAT*-induced promoter activation (Fig 5E). In a chromatin immunoprecipitation (ChIP) assay using anti-*STAT1* antibody, promoters of *cTAZ* and *ISG15* were pulled down in an $\text{IFN-}\alpha$ -sensitive manner, indicating that *STAT1* was recruited to the *cTAZ* and *ISG15* promoters upon $\text{IFN-}\alpha$ stimulation (Fig 5F). The levels of acetylated lysine 27 of histone H3 (H3K27ac), an epigenetic mark of active promoter, around *cTAZ* and *ISG15* promoters were not modulated by $\text{IFN-}\alpha$ (Appendix Fig S4E). Although H3K27ac levels were not modulated by IFN stimulation, it might facilitate the recruitment of *STAT* proteins to target promoters. Taken together, the expression of *cTAZ* is directly induced by *JAK-STAT* signaling to negatively regulate *JAK-STAT* signaling.

In summary, this study has identified a new transcript variant *cTAZ* and revealed its function in modulating the *JAK-STAT* signaling. In the absence of *cTAZ*, *JAK-STAT* signaling can effectively induce expression of ISGs and boost cellular antiviral response. On the other hand, in the presence of *cTAZ*, it will repress the nuclear translocation of *STAT* proteins by inhibiting the dimerization of phosphorylated *STAT1/2* and their subsequent interaction with importin- α 5, which in turn lead to reduced expression of ISGs and antiviral response (Fig 5G). The expression of *cTAZ* is also slightly induced by *JAK-STAT* signaling, and elevated *cTAZ* expression may keep *STAT1/2* activity in check and prevents uncontrolled expression of ISGs and subsequent detrimental effect (Fig 5G). In light of the findings in this study, we envisage that the impact of *cTAZ*-mediated regulation of *JAK-STAT* signaling goes beyond antiviral responses. For instance, *cTAZ* expression may confer resistance to IFN therapy for certain types of cancer [1,2,4]. Conversely, defects in *cTAZ* expression and function may contribute to hypersensitivity to IFNs and autoimmune diseases.

Materials and Methods

Antibodies, plasmids, and other materials

The information about vendor and catalog number of antibodies used in this study is shown in Appendix Table S3.

TAZ, *cTAZ*, *YAP*, *STAT1/2*, and *MAVS* were cloned into pLVX vector. 8 \times GTTC-luciferase reporter and *cTAZ* luciferase reporter were in-house constructed. $\text{IFN-}\beta$ luciferase reporter, 5 \times ISRE-luciferase reporter, and *caRIG-I* were described in [22]. The shRNA plasmids (*YAP*, TRCN0000300325; *TAZ*, TRCN0000370007) were from Sigma-Aldrich.

$\text{IFN-}\alpha$ was purchased from Sino Biological. Primers and oligos (see Appendix Table S4 for sequence information) were synthesized by Huajin Biotech, China.

C57BL/6 wild-type male mice (4 weeks old) were dissected to obtain tissues, proteins, and mRNA. The use of mice for this study was approved by Ethic Committee of Institutes of Biomedical Sciences, Fudan University.

Patient specimens

Lymph nodes near thyroid were collected during surgery, from 11 thyroid cancer patients who were treated at Fudan University Shanghai Cancer Center. Tissue samples were immediately frozen and stored at -80°C for protein extraction, or stored in RNeasy later at 4°C for 24 h and then transferred to -80°C for RNA extraction. Following pathological examination, lymph nodes without cancer metastasis were used in this study. This study was approved by the Ethical Committee of Fudan University Shanghai Cancer Center (050432-4-1212B), and informed consent was obtained from all patients.

Cell culture, transfection, and lentivirus transduction

RKO cells were cultured in RPMI-1640 (Hyclone) containing 10% FBS (Gibco) and 50 mg/ml penicillin/streptomycin (P/S). MCF-10A cells were cultured in DMEM/F12 (Hyclone) supplemented with 5% horse serum (Invitrogen), 0.5 mg/ml hydrocortisone, 20 ng/ml EGF, 10 mg/ml insulin, 100 ng/ml cholera toxin, and 50 mg/ml P/S. Other type cell lines, such as HEK293A, Caco2, ACHN, NCI-H2372, and NCI-H2452, were cultured in DMEM (Hyclone) containing 10% FBS and P/S. All cells were incubated at 37°C under 5% CO_2 .

DNA transfection using PolyJet (SignaGen) was performed according to manufacturer's instructions. Lentivirus was produced by co-transfecting HEK293A cells with viral vectors and packaging plasmids (psPAX.2 and pMD2.G). After 48 h of transfection, lentivirus supernatant was filtered through a $0.45\text{-}\mu\text{m}$ filter, followed by infecting cells together with 5 mg/ml polybrene. One day after infection, the medium was replaced with fresh culture medium containing 1 mg/ml puromycin (Invivogen).

Immunoblotting

Cells were lysed in 1 \times SDS loading buffer containing 50 mM Tris pH 6.8, 2% SDS, 0.025% bromophenol blue, 10% glycerol, and 5% BME. Proteins were resolved by 7.5–10% sodium dodecyl sulfate–polyacrylamide gel electrophoresis (SDS–PAGE) and transferred to PVDF membrane. Membranes were blocked with 5% BSA/TBST or skim milk, incubated with different primary antibodies (4°C , overnight) and HRP-conjugated secondary antibodies. Molecular weight marker, ECL substrates, and image acquisition equipment (5200S) were from Tanon Science & Technology Co., Ltd. If required, ImageJ software was used to facilitate quantification.

Immunofluorescence (IF)

Cells were seeded on fibronectin-coated coverslips, incubated, and treated with condition medium, $\text{IFN-}\alpha$, or virus. Cells were washed with cold PBS, fixed with 4% paraformaldehyde for 15 min, and

permeabilized with 0.2% Triton X-100 at room temperature (RT). After blocking in 3% BSA or 3% goat serum, cells were incubated with first antibodies diluted in 3% BSA for 1.5 h at room temperature or overnight at 4°C. Next, cells were incubated with Alexa Fluor 488- or Alexa Fluor 594-conjugated secondary antibodies (1:1,000 diluted) for 1–2 h, washed, mounted, and subjected to microscopy.

Immunoprecipitation (IP)

Cells were lysed using a mild lysis buffer (MLB) containing 20 mM Tris, 2 mM EDTA, 100 mM NaCl, 1% NP-40, 50 mM NaF, 1 mM Na₃VO₄, and protease inhibitor cocktail (Biotool). Cleared cell lysates were then subjected to IP using various antibodies for 2–4 h. After 3–4 washes with MLB, the proteins were eluted by 1× SDS loading buffer, resolved by SDS-PAGE, and subjected to IB.

GFP fluorescence intensity measurement

Cells were lysed using MLB as mentioned in IP assay, and the fluorescence intensity of cleared lysates was determined by BioTek microplate spectrophotometer at excitation wavelength (485/20) and emission wavelength (528/20).

RNA isolation and qPCR

Total RNA was extracted using the TRIzol reagent (Invitrogen). cDNA was generated by the PrimeScript™ RT Reagent Kit (TaKaRa), and quantitative qPCR was conducted using SYBR Green qPCR Master Mix (TaKaRa) on 7500 Real-Time PCR systems (Applied Biosystems). Relative abundance of mRNA was calculated by normalization to GAPDH mRNA.

Luciferase reporter assay

HEK293A cells were transfected with the indicated reporters (100 ng), control Renilla luciferase reporter (50 ng), and other expression plasmids. After 12 h of transfection, cells were treated with condition medium or IFN for 24 h. Luciferase activity was determined by using a Dual-Luciferase Assay Kit (Promega). Firefly luciferase activity was measured and normalized with co-transfected Renilla luciferase activity.

Soft agar colony formation assay

Agar (1.0%) and 2× DMEM (or RPMI-1640) media were mixed at > 42°C and placed onto 3.5-cm dishes to generate 0.5% base agar. MCF-10A cells (vector, Flag-cTAZ, Flag-TAZ) were seeded in 0.35% top agar (1,000 cells per plate for MCF-10A). Cells were incubated at 37°C with fresh medium replenished regularly for 3 weeks. Cell colonies were counted after staining with crystal violet.

RNA-seq data analysis

Total RNA was extracted from RKO cells (WT, cTAZ^{-/-}, and cTAZ^{-/-} GFP-cTAZ) using RNeasy Mini Kit (Qiagen). The

sequencing libraries were constructed using the TruSeq RNA Sample Prep Kit (Illumina) according to the manufacturer's protocol. Sequencing was performed on an Illumina HiSeq 2500 platform. The differentially expressed genes were identified using DESeq2 [44]. Sequencing reads from RNA-seq data were aligned using the spliced read aligner HISAT2, which was supplied with the Ensembl human genome assembly (Genome Reference Consortium GRCh38) as the reference genome. Gene expression levels (read counts) were calculated using featureCount. All read count data were provided as input to DESeq2 with default parameters. The differentially expressed genes were extracted with fold change ≥ 2 and $P_{\text{adj}} < 0.05$. The Database for Annotation, Visualization, and Integrated Discovery (DAVID) was employed to explore GO ontologies with the differentially expressed genes. Differentially expressed genes are shown in Dataset EV1.

BioID

MCF-10A cells stably express promiscuous biotin ligase (BirA*) tagged GFP, cTAZ, TAZ, or YAP were established. BioID was performed following a published protocol [45]. Briefly, cells (in a 10-cm dish) were treated with biotin (50 μM) for 24 h, washed with PBS twice, and lysed in 600 μl of lysis buffer (50 mM Tris, pH 7.4, 500 mM NaCl, 0.2% SDS, and protease inhibitor). Detergent (20% Triton X-100, 240 μl) was added, and the total lysate was then subjected to sonication to disrupt visible aggregates. The lysate was centrifuged for 10 min at 16,500 $\times g$ at 4°C, and the supernatants were incubated with appropriate amount of streptavidin beads (Thermo) overnight at 4°C. Beads were washed six times with wash buffer. 10% of beads was saved for IB, and the rest was resuspended gently in 50 μl of 50 mM ammonium bicarbonate buffer and subjected for mass spectrometry analysis. Interacting proteins identified are shown in Dataset EV2.

Analysis of public datasets

RNA-seq data were downloaded from the Sequence Read Archive (SRA) (<https://www.ncbi.nlm.nih.gov/sra>), and Galaxy was used for transcript assembly (<https://usegalaxy.org/>). ENCODE ChIP-seq data (HCT-116 and MCF-7 cells) for H3K9ac, H3K27ac, H3K4me1, H3K4me2, and H3K4me3 were mapped to hg19 and visualized using UCSC Genome Browser. Expression datasets for cTAZ and TAZ transcripts in tissues were downloaded from UCSC xena (<https://xenabrowser.net/datapages/>), and TOIL RSEM expected_count datasets were used.

ChIP assay

Chromatin immunoprecipitation (ChIP) assays were performed according to the public protocol [46]. In brief, RKO cells were fixed with 1% formaldehyde for 15 min at room temperature and quenched by adding 1 M glycine (at final concentration of 125 mM) for 15 min. The fixed cells were washed twice with PBS and then were lysed, and chromatin was sonicated into ~500-base pair fragments. IP was performed overnight at 4°C with 2 μg anti-STAT1, anti-H3K27ac or equal amount of mouse IgG for negative control. The second day, protein-G agarose beads were added to the lysates and incubated for 2 h at 4°C. Then, the beads were washed

sequentially with low-salt buffer, high-salt buffer, LiCl buffer, and twice with TE buffer, and DNA was then eluted using 200 μ l of fresh elution buffer. The elutes were reverse-cross-linked using 5 M NaCl at 65°C for 4 h and followed by treatment with RNase A at 37°C for 30 min and proteinase K at 45°C for 1 h to remove RNA and protein, respectively. DNA was extracted using a PCR Purification Kit (Tiangen).

Statistical analysis

All experiments subjected to statistical test were repeated for three times. Statistical analyses were performed using software GraphPad Prism7. Error bars indicate standard deviation (SD); unless otherwise indicated, three independent experimental data were used for Student's *t*-test. $P < 0.05$ was considered as statistically significant ($*P < 0.05$; $**P < 0.01$; $***P < 0.001$).

Data availability

RNA-seq data are available at GEO database (accession number: GSE128257, <https://www.ncbi.nlm.nih.gov/geo/query/acc.cgi?acc=GSE128257>). Other datasets are reported in Datasets EV1 and EV2 and the Appendix Tables S1–S4.

Expanded View for this article is available online.

Acknowledgements

We would like to thank Drs. Justin Wong and Renhua Song (The University of Sydney) for analyzing public datasets, Licheng Sun for technical assistance, and Dr. Steven Plouffe for proofreading of this manuscript. F.X.Y. would like to gratefully acknowledge financial support from the National Natural Science Foundation of China (81622038, 81772965, and 31571479) and Shanghai Municipal Commission of Health and Family Planning (2017BR018).

Author contributions

Conceptualization: CF and F-XY; methodology: CF, JianL, SQ, YL, YZe, PY, ZH, JinL, CD, and SH; formal analysis: CF, SH, CD, KC, and F-XY; investigation: CF, SH, and F-XY; resources: SH, CD, YZh, YW, RD, PX, KC, and F-XY; writing of the original draft: CF; review and editing of the manuscript: CF, KC, and F-XY; supervision: F-XY; and funding acquisition: F-XY.

Conflict of interest

The authors declare that they have no conflict of interest.

References

- Hertzog PJ, Williams BR (2013) Fine tuning type I interferon responses. *Cytokine Growth Factor Rev* 24: 217–225
- Hambleton S, Goodbourn S, Young DF, Dickinson P, Mohamad SM, Valappil M, McGovern N, Cant AJ, Hackett SJ, Ghazal P et al (2013) STAT2 deficiency and susceptibility to viral illness in humans. *Proc Natl Acad Sci USA* 110: 3053–3058
- Le Bon A, Thompson C, Kamphuis E, Durand V, Rossmann C, Kalinke U, Tough DF (2006) Cutting edge: enhancement of antibody responses through direct stimulation of B and T cells by type I IFN. *J Immunol* 176: 2074–2078
- Fuchs SY (2013) Hope and fear for interferon: the receptor-centric outlook on the future of interferon therapy. *J Interferon Cytokine Res* 33: 211–225
- Ronnblom L (2011) The type I interferon system in the etiopathogenesis of autoimmune diseases. *Ups J Med Sci* 116: 227–237
- Bach EA, Aguet M, Schreiber RD (1997) The IFN gamma receptor: a paradigm for cytokine receptor signaling. *Annu Rev Immunol* 15: 563–591
- Veals SA, Schindler C, Leonard D, Fu XY, Aebersold R, Darnell JE Jr, Levy DE (1992) Subunit of an alpha-interferon-responsive transcription factor is related to interferon regulatory factor and Myb families of DNA-binding proteins. *Mol Cell Biol* 12: 3315–3324
- Schindler C, Fu XY, Improta T, Aebersold R, Darnell JE Jr (1992) Proteins of transcription factor ISGF-3: one gene encodes the 91- and 84-kDa ISGF-3 proteins that are activated by interferon alpha. *Proc Natl Acad Sci USA* 89: 7836–7839
- Honda K, Takaoka A, Taniguchi T (2006) Type I interferon [corrected] gene induction by the interferon regulatory factor family of transcription factors. *Immunity* 25: 349–360
- Iwasaki A (2012) A virological view of innate immune recognition. *Annu Rev Microbiol* 66: 177–196
- Gonzalez-Navajas JM, Lee J, David M, Raz E (2012) Immunomodulatory functions of type I interferons. *Nat Rev Immunol* 12: 125–135
- Kawai T, Akira S (2011) Toll-like receptors and their crosstalk with other innate receptors in infection and immunity. *Immunity* 34: 637–650
- Schneider WM, Chevillotte MD, Rice CM (2014) Interferon-stimulated genes: a complex web of host defenses. *Annu Rev Immunol* 32: 513–545
- Honda K, Yanai H, Negishi H, Asagiri M, Sato M, Mizutani T, Shimada N, Ohba Y, Takaoka A, Yoshida N et al (2005) IRF-7 is the master regulator of type-I interferon-dependent immune responses. *Nature* 434: 772–777
- Ivashkiv LB, Donlin LT (2014) Regulation of type I interferon responses. *Nat Rev Immunol* 14: 36–49
- Johnson R, Halder G (2014) The two faces of Hippo: targeting the Hippo pathway for regenerative medicine and cancer treatment. *Nat Rev Drug Discov* 13: 63–79
- Pan D (2010) The hippo signaling pathway in development and cancer. *Dev Cell* 19: 491–505
- Piccolo S, Dupont S, Cordenonsi M (2014) The biology of YAP/TAZ: hippo signaling and beyond. *Physiol Rev* 94: 1287–1312
- Yu FX, Zhao B, Guan KL (2015) Hippo pathway in organ size control, tissue homeostasis, and cancer. *Cell* 163: 811–828
- Liu B, Zheng Y, Yin F, Yu J, Silverman N, Pan D (2016) Toll receptor-mediated hippo signaling controls innate immunity in *Drosophila*. *Cell* 164: 406–419
- Wang S, Xie F, Chu F, Zhang Z, Yang B, Dai T, Gao L, Wang L, Ling L, Jia J et al (2017) YAP antagonizes innate antiviral immunity and is targeted for lysosomal degradation through IKK ϵ -mediated phosphorylation. *Nat Immunol* 18: 1270
- Zhang Q, Meng F, Chen S, Plouffe SW, Wu S, Liu S, Li X, Zhou R, Wang J, Zhao B et al (2017) Hippo signalling governs cytosolic nucleic acid sensing through YAP/TAZ-mediated TBK1 blockade. *Nat Cell Biol* 19: 362–374
- Geng J, Yu S, Zhao H, Sun X, Li X, Wang P, Xiong X, Hong L, Xie C, Gao J et al (2017) The transcriptional coactivator TAZ regulates reciprocal differentiation of TH17 cells and Treg cells. *Nat Immunol* 19: 1036
- Ni X, Tao J, Barbi J, Chen Q, Park BV, Li Z, Zhang N, Lebid A, Ramaswamy A, Wei P et al (2018) YAP is essential for Treg-mediated suppression of antitumor immunity. *Cancer Discov* 8: 1026–1043

25. Zhao B, Wei X, Li W, Udan RS, Yang Q, Kim J, Xie J, Ikenoue T, Yu J, Li L et al (2007) Inactivation of YAP oncoprotein by the Hippo pathway is involved in cell contact inhibition and tissue growth control. *Genes Dev* 21: 2747–2761
26. Dupont S, Morsut L, Aragona M, Enzo E, Giulitti S, Cordenonsi M, Zancanato F, Le Digabel J, Forcato M, Bicciato S et al (2011) Role of YAP/TAZ in mechanotransduction. *Nature* 474: 179–183
27. Yu FX, Zhao B, Panupinthu N, Jewell JL, Lian I, Wang LH, Zhao J, Yuan H, Tumaneng K, Li H et al (2012) Regulation of the Hippo-YAP pathway by G-protein-coupled receptor signaling. *Cell* 150: 780–791
28. Zhao B, Li L, Tumaneng K, Wang CY, Guan KL (2010) A coordinated phosphorylation by Lats and CK1 regulates YAP stability through SCF(-beta-TRCP). *Genes Dev* 24: 72–85
29. Lei QY, Zhang H, Zhao B, Zha ZY, Bai F, Pei XH, Zhao S, Xiong Y, Guan KL (2008) TAZ promotes cell proliferation and epithelial-mesenchymal transition and is inhibited by the hippo pathway. *Mol Cell Biol* 28: 2426–2436
30. Chan SW, Lim CJ, Guo K, Ng CP, Lee I, Hunziker W, Zeng Q, Hong W (2008) A role for TAZ in migration, invasion, and tumorigenesis of breast cancer cells. *Cancer Res* 68: 2592–2598
31. Zhang H, Liu CY, Zha ZY, Zhao B, Yao J, Zhao S, Xiong Y, Lei QY, Guan KL (2009) TEAD transcription factors mediate the function of TAZ in cell growth and epithelial-mesenchymal transition. *J Biol Chem* 284: 13355–13362
32. Schoggins JW, Wilson SJ, Panis M, Murphy MY, Jones CT, Bieniasz P, Rice CM (2011) A diverse range of gene products are effectors of the type I interferon antiviral response. *Nature* 472: 481–485
33. Chen K, Liu J, Liu S, Xia M, Zhang X, Han D, Jiang Y, Wang C, Cao X (2017) Methyltransferase SETD2-mediated methylation of STAT1 is critical for interferon antiviral activity. *Cell* 170: 492–506.e14
34. Stark GR, Darnell JE Jr (2012) The JAK-STAT pathway at twenty. *Immunity* 36: 503–514
35. O'Shea JJ, Schwartz DM, Villarino AV, Gadina M, McInnes IB, Laurence A (2015) The JAK-STAT pathway: impact on human disease and therapeutic intervention. *Annu Rev Med* 66: 311–328
36. Yoneyama M, Kikuchi M, Natsukawa T, Shinobu N, Imaizumi T, Miyagishi M, Taira K, Akira S, Fujita T (2004) The RNA helicase RIG-I has an essential function in double-stranded RNA-induced innate antiviral responses. *Nat Immunol* 5: 730–737
37. Reich NC, Liu L (2006) Tracking STAT nuclear traffic. *Nat Rev Immunol* 6: 602–612
38. Reich NC (2013) STATs get their move on. *JAKSTAT* 2: e27080
39. Chen X, Vinkemeier U, Zhao Y, Jeruzalmi D, Darnell JE Jr, Kuriyan J (1998) Crystal structure of a tyrosine phosphorylated STAT-1 dimer bound to DNA. *Cell* 93: 827–839
40. McBride KM, Banninger G, McDonald C, Reich NC (2002) Regulated nuclear import of the STAT1 transcription factor by direct binding of importin-alpha. *EMBO J* 21: 1754–1763
41. Fagerlund R, Melen K, Kinnunen L, Julkunen I (2002) Arginine/lysine-rich nuclear localization signals mediate interactions between dimeric STATs and importin alpha 5. *J Biol Chem* 277: 30072–30078
42. Hong XX, Carmichael GG (2013) Innate immunity in pluripotent human cells: attenuated response to interferon-beta. *J Biol Chem* 288: 16196–16205
43. Ritchie KJ, Malakhov MP, Hetherington CJ, Zhou L, Little MT, Malakhova OA, Sipe JC, Orkin SH, Zhang DE (2002) Dysregulation of protein modification by ISG15 results in brain cell injury. *Genes Dev* 16: 2207–2212
44. Love MI, Huber W, Anders S (2014) Moderated estimation of fold change and dispersion for RNA-seq data with DESeq2. *Genome Biol* 15: 550
45. Roux KJ (2013) Marked by association: techniques for proximity-dependent labeling of proteins in eukaryotic cells. *Cell Mol Life Sci* 70: 3657–3664
46. Li XY, Biggin MD (2012) Genome-wide *in vivo* cross-linking of sequence-specific transcription factors. *Methods Mol Biol* 809: 3–26